Carbon Dioxide Capture for Storage in Deep Geologic Formations – Results from the CO_2 Capture Project

Capture and Separation of Carbon Dioxide from Combustion Sources

Edited by

David C. Thomas
Senior Technical Advisor
Advanced Resources International, Inc.
4603 Clearwater Lane
Naperville, IL, USA

Volume 1

ELSEVIER
2005

Amsterdam – Boston – Heidelberg – London – New York – Oxford
Paris – San Diego – San Francisco – Singapore – Sydney – Tokyo

Elsevier Internet Homepage – http://www.elsevier.com
Consult the Elsevier homepage for full catalogue information on all books, major reference works, journals, electronic products and services.

Elsevier Titles of Related Interest

AN END TO GLOBAL WARMING
L.O. Williams
ISBN: 0-08-044045-2, 2002

FUNDAMENTALS AND TECHNOLOGY OF COMBUSTION
F. El-Mahallawy, S. El-Din Habik
ISBN: 0-08-044106-8, 2002

GREENHOUSE GAS CONTROL TECHNOLOGIES: 6TH INTERNATIONAL CONFERENCE
John Gale, Yoichi Kaya
ISBN: 0-08-044276-5, 2003

MITIGATING CLIMATE CHANGE: FLEXIBILITY MECHANISMS
T. Jackson
ISBN: 0-08-044092-4, 2001

Related Journals:
Elsevier publishes a wide-ranging portfolio of high quality research journals, encompassing the energy policy, environmental, and renewable energy fields. A sample journal issue is available online by visiting the Elsevier web site (details at the top of this page). Leading titles include:

Energy Policy
Renewable Energy
Energy Conversion and Management
Biomass & Bioenergy
Environmental Science & Policy
Global and Planetary Change
Atmospheric Environment
Chemosphere – Global Change Science
Fuel, Combustion & Flame
Fuel Processing Technology

All journals are available online via ScienceDirect: www.sciencedirect.com

To Contact the Publisher
Elsevier welcomes enquiries concerning publishing proposals: books, journal special issues, conference proceedings, etc. All formats and media can be considered. Should you have a publishing proposal you wish to discuss, please contact, without obligation, the publisher responsible for Elsevier's Energy program:

Henri van Dorssen
Publisher
Elsevier Ltd
The Boulevard, Langford Lane
Kidlington, Oxford
OX5 1GB, UK

Phone: +44 1865 84 3682
Fax: +44 1865 84 3931
E.mail: h.dorssen@elsevier.com

General enquiries, including placing orders, should be directed to Elsevier's Regional Sales Offices – please access the Elsevier homepage for full contact details (homepage details at the top of this page).

ELSEVIER B.V.
Radarweg 29
P.O. Box 211, 1000 AE Amsterdam
The Netherlands

ELSEVIER Inc.
525 B Street, Suite 1900
San Diego, CA 92101-4495
USA

ELSEVIER Ltd
The Boulevard, Langford Lane
Kidlington, Oxford OX5 1GB
UK

ELSEVIER Ltd
84 Theobalds Road
London WC1X 8RR
UK

First edition 2005

Library of Congress Cataloging in Publication Data
A catalog record is available from the Library of Congress.

British Library Cataloguing in Publication Data
A catalogue record is available from the British Library.

ISBN: 0-08-044570-5 (2 volume set)

Volume 1: Chapters 8, 9, 13, 14, 16, 17, 18, 24 and 32 were written with support of the U.S. Department of Energy under Contract No. DE-FC26-01NT41145. The Government reserves for itself and others acting on its behalf a royalty-free, non-exclusive, irrevocable, worldwide license for Governmental purposes to publish, distribute, translate, duplicate, exhibit and perform these copyrighted papers. EU co-funded work appears in chapters 19, 20, 21, 22, 23, 33, 34, 35, 36 and 37. Norwegian Research Council (Klimatek) co-funded work appears in chapters 1, 5, 7, 10, 12, 15 and 32.

Volume 2: The Storage Preface, Storage Integrity Preface, Monitoring and Verification Preface, Risk Assessment Preface and Chapters 1, 4, 6, 8, 13, 17, 18, 19, 20, 21, 22, 23, 24, 25, 26, 27, 28, 29, 30, 31, 32, 33 were written with support of the U.S. Department of Energy under Contract No. DE-FC26-01NT41145. The Government reserves for itself and others acting on its behalf a royalty-free, non-exclusive, irrevocable, worldwide license for Governmental purposes to publish, distribute, translate, duplicate, exhibit and perform these copyrighted papers. Norwegian Research Council (Klimatek) co-funded work appears in chapters 9, 15 and 16.

♾ The paper used in this publication meets the requirements of ANSI/NISO Z39.48-1992 (Permanence of Paper).
Printed in The Netherlands.

Carbon Dioxide Capture for Storage in Deep Geologic Formations, Volume 1
D.C. Thomas and S.M. Benson (Eds.)

SELF-ASSEMBLED NANOPOROUS MATERIALS FOR CO_2 CAPTURE PART 2: EXPERIMENTAL STUDIES

Ripudaman Malhotra[1], Albert S. Hirschon[1], Anne Venturelli[1], Kenji Seki[2], Kent S. Knaebel[3], Heungsoo Shin[3] and Herb Reinhold[3]

[1]Chemical Science and Technology Laboratory, SRI International, Menlo Park, CA 94025, USA
[2]Osaka Gas Co., Ltd., Osaka 554, Japan
[3]Adsorption Research Inc., Dublin, OH 43016, USA

ABSTRACT

Adsorption tests verified the expected high capacity of copper terephthalate complex for adsorbing CO_2. The CO_2 isotherm did not level off up to CO_2 partial pressures of 25 psig. The selectivity of the material for CO_2 over N_2 is about 8. Analogous tests with a silicalite (Hisiv 3000) showed saturation behavior above CO_2 partial pressures of 10 psig. Based on laboratory measurements and simulations, a PSA process was designed to capture the CO_2 from a 400 MW gas-fired power plant that would meet the specifications of 90% capture and 96% CO_2 purity. Because pressurizing the total plant exhaust (1586.1 MMSCFD) would place a very high parasitic load (about 260 MW), we opted for a design in which the beds are charged at the pressure of the exhaust, and the CO_2 product is recovered by pulling vacuum. The highest purity obtained in the experiments was 67.9% CO_2 with 34.1% recovery. The production rate was 0.0113 sL/min. Additional simulations of the PSA process revealed that CO_2-rich product with 97% purity is achievable by a 2-bed/5-step PSA process using the copper terephthalate adsorbent; however, it would require a long rinse (with part of the CO_2-rich stream) and purging at low absolute pressure to obtain a high-purity CO_2-rich product.

A rough economic analysis, accounting for capital and power consumption of the PSA system, gave estimated costs, per ton of CO_2 captured, of $406 for the powdered copper terephthalate adsorbent, $495 for the granulated material, and $393 for UOP Hisiv 3000. Considering that the former adsorbents were experimentally obtained from batch syntheses and were not optimized, it is likely that they show good potential for this application, relative to the existing commercial product.

The most striking result though was that the power requirements for CO_2 capture are enormous, about 1 GW or more than twice that of the power plant for which this capture system was being designed. It did not matter whether the adsorbent was copper terephthalate or Hisiv 3000, although it should be pointed out that under the operating conditions, the benefits of the large capacity of copper terephthalate were not being realized. In any case, in order to meet the stipulated requirements, the adsorbent for a PSA-based system must be able to deliver about two orders of magnitude better performance. That goal seems unlikely, and other scenarios in which some of the constraints are relaxed should also be considered.

INTRODUCTION

In the accompanying chapter (Part 1), we described results from the theoretical phase of our project. We made the case that use of copper dicarboxylate salts could substantially reduce the size of a PSA system for capturing CO_2. Our original plan called for synthesizing and testing many variants of these complexes by systematically varying the dicarboxylic acids as well as varying structural features to enhance the binding energy. These variations result in cavities of different sizes, and thereby offer the opportunity to

optimize the adsorption characteristics. However, at the start of this phase, we found out that we had only 9 months to conduct an experimental study that must include a process design and an estimate for the cost of capturing CO_2 from flue gas of gas-fired power plant. We, therefore, focused on a single compound, with the objective of determining its adsorption characteristics as well performing laboratory-scale PSA tests to get sufficient data that would allow us to design a process. We present here results from our studies on a 3D complex of copper terephthalate pillarized with triethylenediamine (TED), a compound that we had examined briefly by molecular modeling.

EXPERIMENTAL SECTION

Synthesis of Materials

The synthesis of the complex consists of two steps. In Step 1, a 2D complex of copper terephthalate is formed by the reaction of copper sulfate and terephthalic acid. This 2D complex is then pillarized with TED to give the 3D complex. A typical synthesis consists of dissolving $CuSO_4{\cdot}(H_2O)_5$ in methanol, and terephthalic and formic acids in DMF, followed by slow addition of the copper solution to the acid solution. The mixture is left standing at 50 °C over a period of several days, over which time a 2D complex of copper terephthalate crystallizes out. The crystals are then heated to 160 °C with TED in toluene in an autoclave to form the 3D complex. The product is an aqua-green powder consisting mostly of particles of cubic morphology and size ranging between 1 and 3 μm. The BET surface areas of the products were in excess of 600 m^2/g with greater than 90% of the area in pores less than 20 Å. The powders were used as such in the static tests, but for dynamic tests they were pressed in pellets, crushed, and sieved to get coarse granules so as to minimize the pressure drop across the adsorption tube.

Static Adsorption Tests

The apparatus for measuring the adsorption isotherms is shown in Figure 1. The adsorbent is loaded into the B cell inside a 25 μm filter. We measured the solid density of the powder by pulling a vacuum on the entire cell. The assumption is that none of the helium is adsorbed by the adsorbent but it can reach all of the pores. The solid density is needed for calculating the isotherm. Determination of each point on the isotherm uses the same basic procedure as measuring the solid density.

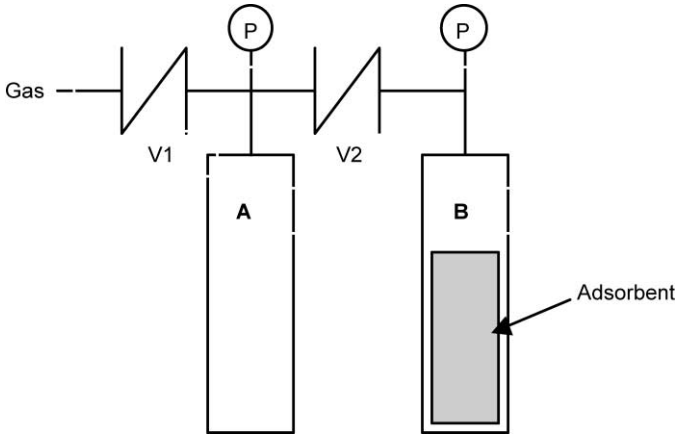

Figure 1: Apparatus for static adsorption tests to determine isotherms.

Breakthrough Measurements

The experimental apparatus is shown in Figure 2. A Perkin-Elmer MGA-1200 process mass spectrometer was used to detect the gas compositions in real-time. Each experiment simulated a complete PSA cycle. The column was pressurized with dry N_2 through valve 1. During pressurization, the feed flow was sent through

valve 4 to allow the feed flow controllers to stabilize and to confirm the CO_2 concentration using the mass spectrometer. Next, the feed was directed through the column via valves 5 and 3 and the column pressure was maintained near atmospheric pressure.

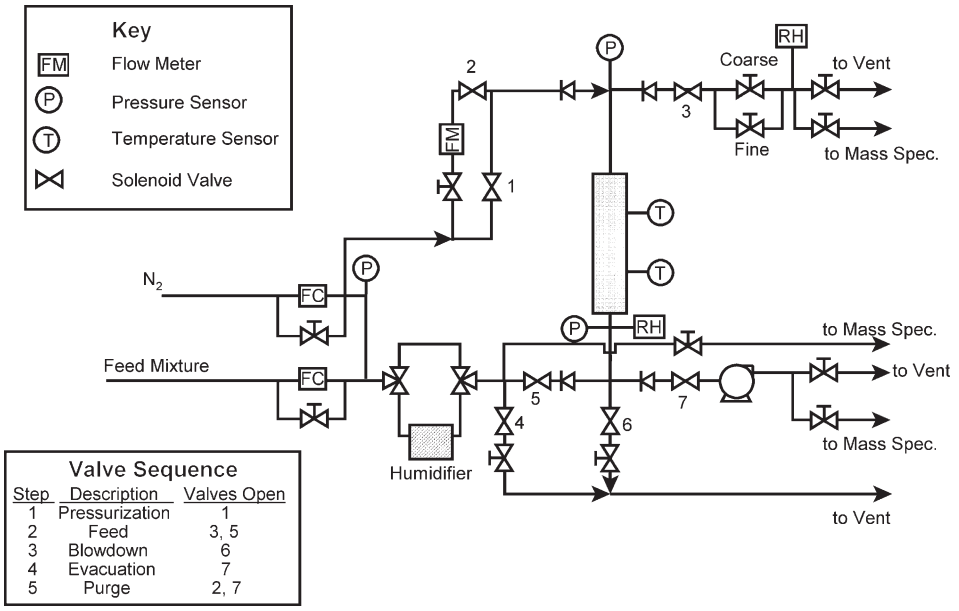

Figure 2: Schematic of apparatus for breakthrough measurements.

The breakthrough experiments were conducted at 30 °C, and the pressure during the feed and purge steps were approximately atmospheric pressure and 10.3 kPa (1.5 psia), respectively. The feed flow rate (superficial velocity) was systematically varied among the experiments between 10, 30, and 100 ft/mm. Two tests, both of which employed the column containing a desiccant layer, examined humidified feed at about 85% RH and 30 °C. Two additional tests examined the effect of a rinse step on a potential PSA cycle. A rinse step provides a means to achieve high carbon dioxide concentration, while an ordinary PSA cycle might only achieve an enrichment from 2 × to 4 × the feed concentration.

The column used was a 2.54 cm (1.0 in.) OD, 316 SS tube with an ID of 2.12 cm (0.835 in.) and 30.48 cm (12 in.) length. For all of the experiments, the column was heated to 30 ± 1 °C with a heating tape. The column pressure was maintained as close to atmospheric pressure as possible while maintaining the proper feed flow rate. The purge flow rate was held constant at 0.11 sL/min.

Lab-Scale Pressure Swing Adsorption

A schematic diagram of the lab-scale 2-bed/5-step PSA system is shown in Figure 3. The beds (2.54 cm (1 in.) OD × 30.48 cm (12 in.) length) were loaded with layered adsorbents. The volumetric ratio of copper terephthalate granules to silica gel (Sorbead AF 125) was 75:25, as for the layered-bed breakthrough tests. Three identical PVC tanks (10.16 cm (4 in.) OD × 30.48 cm (12 in.) length) were used as feed and product tanks. The PSA cycle (valve switching) was controlled and data (time, pressure, concentrations, etc.) were acquired in real-time by a PC running *iFIX* process automation software (Intellution). Gas compositions were analyzed by a mass spectrometer (Perkin Elmer MGA 1200). The feed flow rate and its composition were controlled by mass flow controllers (Unit Instruments) and the product flow rates were controlled by metering valves.

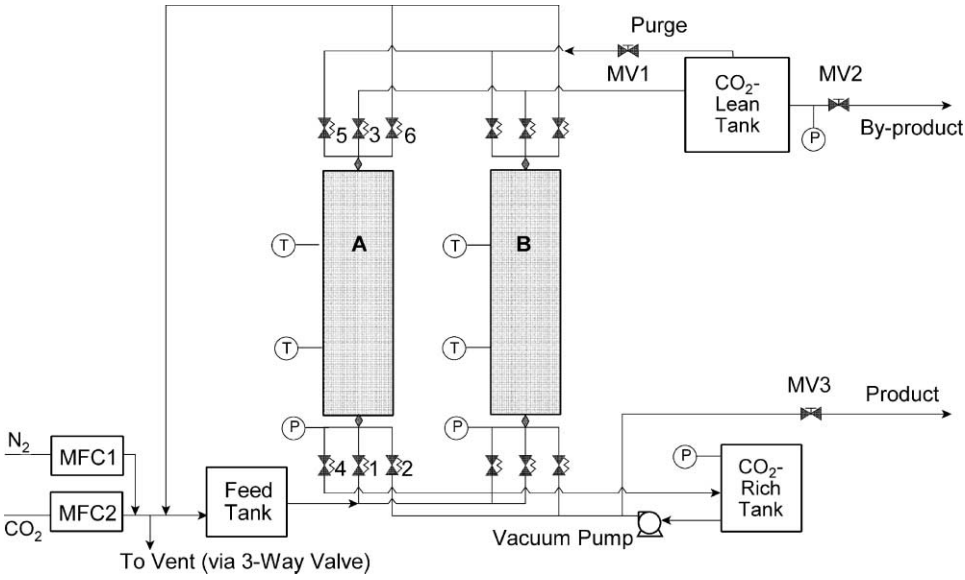

Figure 3: Schematic diagram of 2-bed PSA system.

The step sequence for the PSA cycle considered in this work was carried out in two parallel beds, operated 180-out-of-phase:

2-bed/5-step cycle	
Step	**Description**
1	Feed at P_H
2	Rinse with CO_2-rich product at P_H
3	Evacuation to P_L
4	Purge with N_2-rich product at P_L
5	Pressurize with N_2-rich product to P_H

During the feed step, N_2-rich product was produced by introducing a feed to a bed. In contrast, CO_2-rich product was obtained during steps 3 and 4. A standard linear-driving force based model was used to predict the performance of the PSA system[1].

RESULTS AND DISCUSSION

Static Adsorption Tests

Measurements were made on two different preparations of the 3D complex powder (#54, and #67), granules from one of these samples (#67), and Hisiv 3000 (a reference zeolite). Adsorbent physical property measurements reveal gross differences between adsorbents, and they include, when appropriate: (1) solid density, (2) particle density, (3) bulk density, (4) total void fraction, (5) intraparticle void fraction, (6) interstitial void fraction, (7) specific pore volume, and (8) particle size. Values are summarized in Table 1.

TABLE 1
SUMMARY OF ADSORBENT PHYSICAL PROPERTIES

Form	Density (g/cm^3)			Overall void fraction	Particle void fraction	Specific pore volume (cm^3/g)	Sauter mean particle size (mm)
	Solid	Bulk	Particle				
SRI-54-A	1.692	0.293	–[a]	0.827	–[a]	–[a]	–[a]
SRI-67-A	1.679	0.239	–[a]	0.827	–[a]	–[a]	–[a]
Granules (67)	1.763	0.494	0.916	0.720	0.480	0.524	1.58
Hisiv 3000	2.430	0.648	1.098	0.733	0.548	0.499	2.82

[a] These properties could not be estimated reliably for the adsorbent in its powdered form.

Figure 4 contains the isotherm data and fits for adsorption of N_2 and CO_2 on various adsorbents at 30 and at 100 °C. Not surprisingly, there is greater adsorption of CO_2 than N_2 and both gases are adsorbed to a greater extent at 30 °C than at 100 °C. There is no significant difference between the copper terephthalate samples. It is noteworthy that whereas the adsorption isotherm of CO_2 on silicalite shows a curvature indicative of saturation, the corresponding isotherms for copper terephthalate show no such leveling off even at higher pressures, which is a direct consequence of their high overall capacity. However, the advantage of copper terephthalate crystals manifests itself only at CO_2 pressures greater than 100 kPa (~15 psi). With a concentration of only 4% in the flue gas, the partial pressure of CO_2 will exceed 100 kPa at total pressures greater than 2.5 MPa (25 atm). Furthermore, the heat of adsorption for CO_2 from measurements at these two temperatures is calculated to be only 19.7 kJ/mol (4.7 kcal/mol), a value that is substantially lower than our target of ca. 30 kJ/mol (7 kcal/mol).

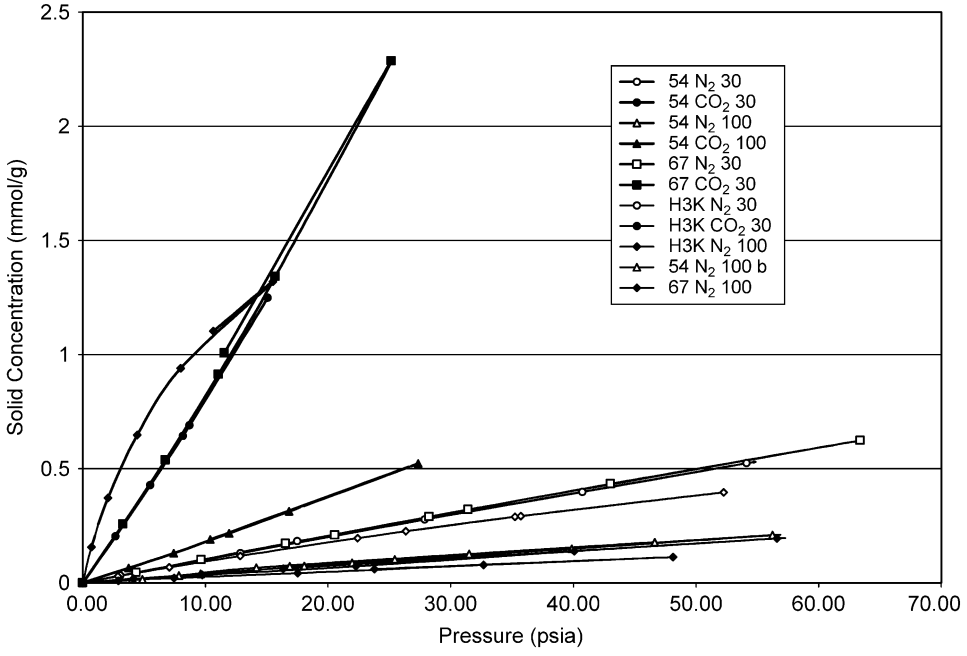

Figure 4: Adsorption isotherms for CO_2 and N_2 over various substrates at 30 and 100 °C.

Table 2 lists the isotherm parameters obtained by fitting the raw data. The table also includes values for the granules. The Henry's law constant for the granules is significantly lower than for the powder materials. The drop in performance of granules is a reminder of the importance of proper engineering of meso and macropores in addition to the micro (or nano) pores. Selectivities, which indicate relative adsorbability, were estimated from the ratios of Henry's law coefficients. The first type was: $\alpha_{CO_2-N_2} = A_{CO_2}/A_{N_2}$. Obviously, the higher the value, the more strongly adsorbed is the component in the numerator. The second type of selectivity accounts for the most significant adsorbent–adsorbate properties with regard to pressure swing adsorption applications. It is given by:

$$\beta_{CO_2-N_2} = [1 + ((1 - {}'\Omega)/{}'\Omega)A_{CO_2}]/[1 + ((1 - {}'\Omega)/{}'\Omega)A_{N_2}]$$

Values for these parameters are listed in Table 3. For silicalite data the "A" parameters for the Langmuir isotherms were compared.

TABLE 2
ISOTHERM PARAMETER SUMMARY (UNITS OF PSIA VERSUS MMOL/G)

Adsorbent	**Henry's Law (30 °C)**	**Langmuir (30 °C)**		**Henry's Law (100 °C)**	**Langmuir (100 °C)**	
	A	***A***	***B***	***A***	***A***	***B***
CO_2						
SRI-54-A	0.08094			0.01877		
SRI-67-A	0.08798			0.02152		
Granules (67)	0.04533			n.a		
Hisiv 3000		0.20914	0.09502		0.04264	0.03452
N_2						
SRI-54-A	0.00980			0.00379		
SRI-67-A	0.01002			0.00344		
Granules (67)	0.00639			n.a		
Hisiv 3000		0.00991	0.00594		0.00265	0.00271

TABLE 3
ADSORBENT COMPONENT SELECTIVITIES AT HENRY'S LAW LIMIT

Adsorbent	$\alpha_{CO_2-N_2}$		$\beta_{CO_2-N_2}$	
	30 °C	**100 °C**	**30 °C**	**100 °C**
SRI-54-A	8.26	4.96	0.310	0.592
SRI-67-A	8.78	6.25	0.291	0.541
Granulated disks	7.09	n.a	0.325	n.a
Hisiv 3000	21.10	16.12	0.101	0.241

The selectivity, $\alpha_{CO_2-N_2}$, represents the main characteristic of the isotherms with regard to the ability to separate the components. The *higher* the numerical value, the better the expected performance. In contrast, the selectivity, $\beta_{CO_2-N_2}$, represents the isotherms and adsorbent voidage, both of which are critical to PSA performance. In this case, the *lower* the numerical value, the better the expected performance, though inherent kinetics are important. The values for $\alpha_{CO_2-N_2}$ and $\beta_{CO_2-N_2}$ are similar for both powdered forms of copper terephthalate. The granules, however, exhibited a decrease in separating capability since $\alpha_{CO_2-N_2}$

was smaller, and $\beta_{CO_2-N_2}$ was larger than for the powdered materials. In contrast, the values for Hisiv 3000 indicate that it is a better adsorbent from an equilibrium standpoint, since $\beta_{CO_2-N_2}$ was smaller, and $\alpha_{CO_2-N_2}$ was larger than for both forms of copper terephthalate.

In addition to equilibrium tendencies, time dependence or *kinetics* also plays a role in adsorption processes. Slow kinetics can prevent an adsorbent from achieving its full potential, which would lead to larger and less efficient equipment. We observed that whereas the kinetics was rapid for the powder samples, the granules that we prepared take a substantially longer time to equilibrate. Water isotherm measurements were performed to see how the adsorption of CO_2 was affected by humidity. All of the adsorbents exhibited low capacity for moisture at low RHs (e.g. <0.03 g_{H_2O}/g_{Ads} at 36% RH). In contrast, the moisture capacity of the copper terephthalate adsorbents increased significantly at relative humidities $>42.5\%$ RH (>0.07 g_{H_2O}/g_{Ads}). Conversely, at higher humidities ($>50\%$ RH), the capacity for moisture of Hisiv 3000 is significantly lower (<0.05 g_{H_2O}/g_{Ads}) compared to the copper terephthalate adsorbents.

Breakthrough Measurements

Figure 5 shows an example of the composition and temperature histories for the entire cycle. Vertical lines separate the different steps. Composition was measured at three different points in the process. Those sample points were connected to individual inlets of the mass spectrometer. The composition dips shown in Figure 4 at the beginning of the feed step and the beginning of the evacuation step are due to switching between the inlet ports, e.g. at the beginning of the test and at about 105 s.

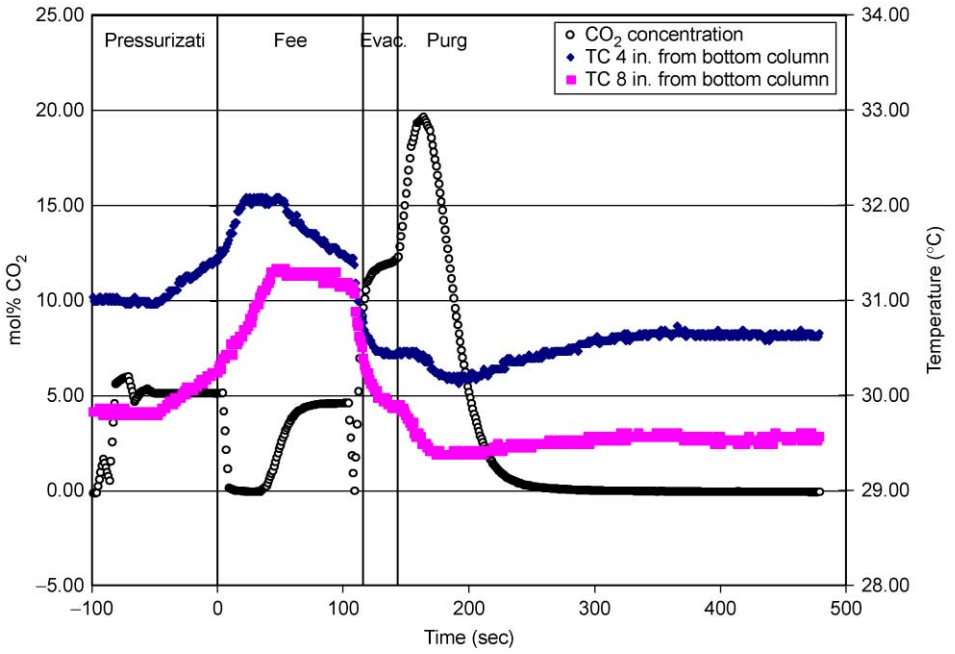

Figure 5: CO_2 concentration and temperature versus time.

Both thermocouples indicate that a temperature rise occurs during pressurization. This rise is due to uptake of nitrogen, which was admitted slowly so as not to over-pressurize the column before beginning the feed step. Subsequently, the temperature profiles exhibit a change in slope near the beginning of the feed step, due to the heat of adsorption of carbon dioxide. Once the CO_2 front passed each thermocouple, the adsorbent began to cool.

Tests were conducted with beds packed either with granulated copper terephthalate alone (Column 1) or with a layer of silica followed by copper terephthalate (Column 2). Figure 6 shows the raw data collected during the test in the form of CO_2 concentration versus time t, where $t = 0$ is the beginning of the feed step for a test with Column 1. The higher the flow rate, the earlier the breakthrough occurred. The replicate tests at 10 ft/min show good repeatability. Integration of these data, yields the stoichiometric breakthrough time, t_{Stoich}. That is, the area below the breakthrough curve from $t = 0$ to t_{Stoich} equals the area above the breakthrough curve from t_{Stoich} until the time at which the product concentration rises to that of the feed. Data were also collected for breakthrough from Column 2 and when the feed gas was humidified. The stoichiometric breakthrough time as well as the amount of gas fed until that time have been calculated. The amount of purge gas required divided by the amount of gas fed at t_{Stoich} was also determined. Analyses of these data show that for dry feed gas, the granular copper terephthalate adsorbent had a slightly greater capacity for CO_2 than the two-layer bed, also with dry feed gas. When the feed gas was humidified, however, the two-layer bed had a higher capacity than when it was dry, though not quite as high as the copper terephthalate alone, exposed to dry feed gas.

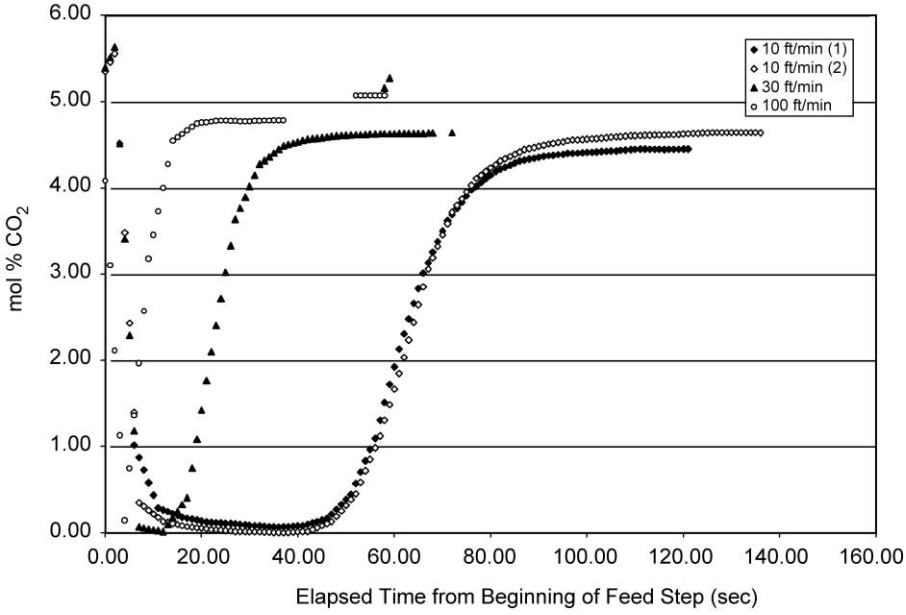

Figure 6: CO_2 concentration versus time for tests using Column 1.

Laboratory PSA Tests and Simulations

The data from static and breakthrough tests were used to design the lab PSA test cycle and simulations. A breakthrough test was simulated prior to attempting to simulate PSA performance, in order to confirm the validity, the model and parameters. The breakthrough test consisted of the following sequence of steps: feed (101 s), evacuation (4 s) and purge (290 s). In the breakthrough test, the bed was packed only with SRI 54 adsorbent. Essential data (e.g. pressure, composition, and flow rate versus time) were collected in order to properly set the initial and boundary conditions of the simulation. The simulation results, shown in Figure 7 agree fairly well with the experiment, although there is a slight quantitative discrepancy during the evacuation and purge steps.

The experimental data exhibit lower capacity than estimated by the simulation. That is evidenced in the premature breakthrough (at about 50 s) during the feed step, and a shallower and less broad peak in

the blowdown and purge steps, from about 100 to 210 s. Part of the discrepancy, however, may have been due to inaccurate flow rate measurements, which would distort the apparent times.

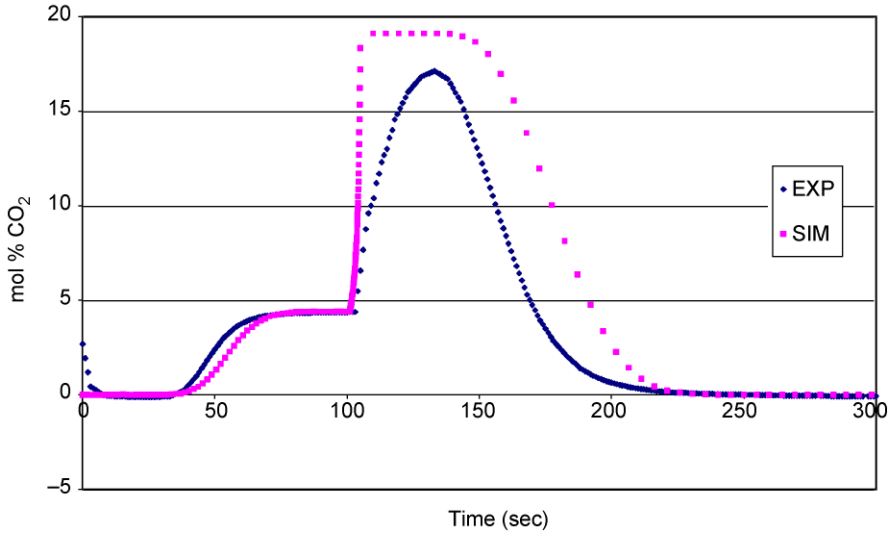

Figure 7: Comparison of experimental data and simulation breakthrough test. Feed $P = 15.9$ psia; Eva $P = 2.3$ psia; $T = 30$ °C; Ads. Mass = 58.87 g of SRI-54.

Simulation results

The simulation model was also used to predict the effect of various parameters on the performance. The findings are as follows:

Effect of rinse amount. Increasing rinse resulted in higher purity of the CO_2-rich product and higher CO_2 recovery, but a lower CO_2 production rate. In contrast, the feed flow rate decreased and more power (for vacuum) was required.

Effect of purge amount. Excessive purging resulted in higher CO_2 recovery and a higher CO_2 production rate, but with lower CO_2 purity. In addition, the purity of the N_2-rich product increased. In contrast, the required feed flow rate and required power (for vacuum) were not affected significantly.

Effect of feed amount. Excessive feed caused significantly lower CO_2 recovery, in addition to a lower CO_2 production rate. In addition, the purity of the N_2-rich product decreased. In contrast, the CO_2 concentration in the main product and the required power (for vacuum) were not affected.

Effect of evacuation pressure. PSA performance depends rather strongly on the ratio of absolute pressures in the cycle. Hence, the evacuation pressure is expected to play a significant role. In this case study, an evacuation pressure of 20 kPa (0.2 bar) was compared with that of 10 kPa (0.1 bar). At 20 kPa, it was not possible to obtain high CO_2 concentrations for the main product. The maximum purity was about 91%. In contrast, as noted previously, the CO_2 concentration at 10 kPa was as high as 96.6%. In addition, at 20 kPa, the CO_2 recovery, the CO_2 production rate, and the purity of the N_2-rich product all decreased. The only advantage was that the power consumption (for vacuum) was reduced.

Cycle tests

In these tests, as for the simulations, the effects of feed and purge amounts were examined to find an optimal operating condition. The purge amount was controlled by a metering valve (MV1 in Figure 3) in the purge line. The test conditions and results are listed in Tables 4 and 5, respectively.

TABLE 4
EXPERIMENTAL PSA TEST CONDITIONS

Test no.	Feed			Evacuation pressure (psia)	Purge pressure (psia)	Opening of purge valve (turn)
	Flow (sL/min kg)	Composition (CO_2% in N_2)	Pressure (psia)			
1	22.67	4.18	17.7	2.4–3.5	3.5–4.0	7
2	6.167	4.15	15.8	2.0–3.2	3.2–3.4	7
3	4.637	4.23	15.6	2.1–3.2	3.2–3.5	7
4	6.167	4.15	16.1	2.4–3.6	3.6–4.4	10
5	6.167	4.15	16.1	2.3–3.8	3.8–4.8	13
6	6.167	4.15	16.2	2.3–4.1	4.1–5.0	15

TABLE 5
EXPERIMENTAL PSA RESULTS

Test no.	CO_2-rich product			N_2-rich product	
	Purity (% CO_2)	CO_2 recovery (%)	Production rate (sL/min kg)	Purity (% CO_2)	Production rate (sL/min)
1	48.9	8.7	0.1700	2.3–4.8	22.67
2	56.9	30.1	0.1380	2.48–5.29	5.97
3	56.4	29.9	0.1043	2.22–4.65	4.51
4	63.1	31.0	0.1258	2.2–5.5	6.29
5	67.9	34.1	0.1281	2.16–6.2	6.16
6	38–64	19.7	0.0964	2.12–6.1	6.19

In the first set of tests (Tests 1–3), the feed amount was reduced systematically. The results indicate that excessive feed led to low CO_2 recovery (Test 1). In contrast, too little feed resulted in a lower production rate of CO_2 (Test 3). Thus, the feed amount in Test 2 was maintained for the subsequent set of tests.

In the next set of tests (Tests 2, 4–6), the amount of purge was varied. In this case, there is an optimum purge amount (Test 5), which led to high CO_2 purity of 67.9%. In contrast, excessive purge (Test 6) resulted in lower CO_2 purity, with oscillating behavior, possibly due to incomplete mixing of effluent in the product tank. In addition, the high purge flow raised the pressure during the evacuation and purge steps, resulting in inferior performance.

The CO_2 purity of the main product in the experimental PSA tests was significantly lower than that achieved in the simulations. One reason for this discrepancy might be that the experimental pressure during evacuation and purge was higher than in the simulations. This was a drawback of the limited apparatus (and short time available). Although the pressure of the CO_2 product tank reached 18.5 kPa (0.165 bar) during phases when no effluent from either bed was being admitted to the tank, the pressure increased above 20 kPa during evacuation and it became even higher during the purge step.

According to the simulations, at an evacuation pressure of 20 kPa, the maximum CO_2 purity was reduced from 97 to 91% at 10 kPa. As a result, the achievable purity would be lower at a pressure above 20 kPa.

Summary of PSA tests and simulations
The results from the tests and simulations can be summarized as follows:

1. Simulation of a breakthrough test with the model and adsorbent parameters obtained from batchwise measurement described fairly well the experimental results.
2. Case studies examined the feasibility of capturing CO_2 from a dry flue gas via numerical simulations.
3. It is possible to obtain a CO_2-rich product having a purity of 97% by a 2-bed/5-step PSA process using copper terephthalate adsorbent.
4. Effects of important operating parameters were examined and optimized.
5. Sufficient rinse and vacuum is essential for obtaining high CO_2 purity.
6. Excessive purge reduced the CO_2 purity of the main product. In addition, excessive feed resulted in a low recovery of CO_2.
7. A 2-bed PSA unit was built and the 5-step cycle was tested for CO_2 capture from a simulated flue gas mixture of 4% CO_2 in N_2.
8. The optimum feed and purge amounts were observed in two sets of tests.
9. The best experimental result was 67.9% CO_2 in the main product at 34.1% recovery and at a production rate of 0.0113 sL/min.
10. The relatively low CO_2 purity in the experiments was due to high pressure during the evacuation and purge steps, and to a high production rate.

Process Cost Estimation
A rough economic analysis was performed to estimate the cost of capturing CO_2 from a 400 MWe gas-fired turbine. Both experimental results and projections obtained from the mathematical model were used to make this estimate. As stated earlier, the model results were based on the experimental data along with the governing material balance and constitutive equations. Using the conditions provided by the CCP, the simulator was run to simulate operation of a full-scale system, i.e., to handle 78,912 kg mol/h at a CO_2 mole fraction of 0.04. The flow rate amounts to 1586.1 MMSCFD feed (million std. cubic feet per day; 44.913×10^9 sL/day). The economic analysis accounted for the capital and power consumption of the PSA system. In order to do that, it was necessary to know the amount of gas that flowed into and out of the beds for each step, along with the relevant pressures, times, etc. That information was obtained from the simulation results.

The beds for the powdered copper terephthalate adsorbent properties were found to be 2,880,996 kg/bed, while the granulated material required 5,548,676 kg/bed. In contrast, a design based on UOP Hisiv 3000 (silicalite) required 1,440,498 kg/bed. By accounting for the adsorbers and other vessels, vacuum pumps (which are expected to be enormous compared with those commonly available), valves, controls, and power, along with labor, installation, and a modest margin, the estimated costs per ton of CO_2 captured were: $406.51 for the powdered copper terephthalate adsorbent, $494.88 for the granulated material, and $393.12 for UOP Hisiv 3000. Prohibitively expensive as they are, these costs do not yet account for amount of power consumed. The estimated power consumption to capture CO_2 from this 400 MWe plant was in the order of 1 GWe.

In retrospect, these values are not surprising. The benefits of the high capacity of the copper terephthalate system are not realized at low partial pressures of CO_2 (Figure 4). Indeed, at low pressures, silicalite had a slightly higher capacity. It is interesting to note that our estimate for power requirements is on the same order as that of Halmann and Steinberg, who report requiring 700 MWe to capture CO_2 from a 1000 MWe coal-fired plant [2]. This result only emphasizes the importance of choosing an appropriate application. Clearly, this material is not suitable for cases where the partial pressure of CO_2 is less than 10 psi. An oxygen-fired coal gasification combined cycle power plant would be better suited to take advantage of this material because it has a higher concentration of CO_2 and the CO_2 separation could be performed at a stage when the gases are still in the compressed state.

CONCLUSIONS

In static tests, we have shown that the 3D copper terephthalate complex absorbs CO_2 at room temperature, and because there was no leveling off in the isotherm at the highest pressures tested, the 3D complex appears to have a very high capacity. High capacity is important because it reduces the overall size of the bed and the attendant compressors of a PSA system, and directly reduces the capital and operating expenses.

We made pressed disks from the 3D complex for the dynamic tests to monitor the breakthrough of CO_2 through packed beds. The disks retain their integrity during normal handling and shipping and thus appear to have adequate mechanical strength for use in a packed bed. The breakthrough tests helped us design a laboratory PSA system, whose performance was used to design a full-scale system. Capital and operating expenses for this full-scale system were estimated and found to be prohibitive for capturing CO_2 from a 400 MWe gas-fired turbine power plant.

NOMENCLATURE

A	Henry's Law (or Langmuir) coefficient
B	Langmuir's coefficient
BET	Brunauer Emmett Teller
CCP	CO_2 Capture Project
DMF	*N*,*N*-Dimethylformamide
PSA	Pressure swing adsorption
TED	Triethylene diamine (also known as [2,2,2,]diazabicyclooctane)
MMSCFD	Million standard cubic feet per day
P_H	Upper absolute pressure of PSA cycle
P_L	Lower absolute pressure of PSA cycle
PVC	Polyvinylchloride
MW	Megawatt
MWe	Megawatt electric
GWe	Gigawatt electric
RH	Relative humidity
α	Selectivity (ratio of Henry's Law coefficients)
β	Selectivity (ratio of Column isotherm slopes)
$'\Omega$	Overall void fraction
t_{Stoich}	Stoichiometric breakthrough time

ACKNOWLEDGEMENTS

We acknowledge many fruitful discussions with Drs Piergiorgio Zappelli and Daniel Chinn during the course of our project that helped clarify our concepts.

REFERENCES

1. D.M. Ruthven, S. Farooq, K.S. Knaebel, Pressure Swing Adsorption, VCH Publishers, New York, NY, 1994.
2. M.M. Halmann, M. Steinberg, Greenhouse Gas Carbon dioxide Mitigation, Lewis Publishers, Washington, DC, 1999.